PSEUDO REVERSIBLE SYMMETRIC EXTENSION FOR LIFTING-BASED NONLINEAR-PHASE PARAUNITARY FILTER BANKS

Taizo Suzuki[1], *Naoki Tanaka*[2], *and Hiroyuki Kudo*[1]

1: Faculty of Engineering, Information and Systems, University of Tsukuba, Japan
2: Department of Computer Science, University of Tsukuba, Japan
Email: taizo@cs.tsukuba.ac.jp, tanaka@imagelab.cs.tsukuba.ac.jp, and kudo@cs.tsukuba.ac.jp

ABSTRACT

This study presents a pseudo reversible symmetric extension (P-RevSE) that solves the signal boundary problem of lifting-based nonlinear-phase paraunitary filter banks (L-NLPPUFBs), which have high compression rates thanks to their not having a constraint on the linear-phase property unlike the existing transforms used in image coding standards. The conventional L-NLPPUFBs with a periodic extension (PE) yield annoying artifacts at the signal boundaries. However, the P-RevSE is implemented smoothly at the signal boundaries by using a nonexpansive convolution of a symmetric extension (SE) and determinant control for the lifting factorization. Although the determinant control causes a *pseudo* SE, not a *true* SE, the resulting L-NLPPUFB with P-RevSE outperforms not only the L-NLPPUFB with PE but also the current transform used in JPEG XR.

Index Terms— Lifting structure, lossy-to-lossless image coding, nonlinear-phase paraunitary filter bank, signal boundary problem, symmetric extension.

1. INTRODUCTION

Image compression (coding) standards help to alleviate the burden on servers and free up communication bandwidth. JPEG is the most common image coding standard, but it uses the discrete cosine transform (DCT), which causes blocking artifacts in low bitrate compression. JPEG XR (eXtended Range) [1] is a more effective image coding standard that uses a lapped transform (LT) [2], which is a class of linear-phase filter banks (LPFBs) [3], and it solves the blocking problem. Although LPFBs have to extend the signals at the signal boundaries because of the overlapping processing, the output signals should not be larger than the input signals. A periodic extension (PE), which is one of the simplest boundary processing, causes annoying artifacts due to discontinuities at the signal boundaries. LPFBs solve the problem by using a symmetric extension (SE) [4], which extends the boundary signals smoothly and does not require transmission of extra signals for reconstruction.

Nonlinear-phase filter banks (NLPFBs) [5, 6] have high compression rates thanks to their not having a constraint on the linear-phase property unlike LPFBs. NLPFBs also have the signal boundary problem, and some solutions for it have been presented [7–10]. On the other hand, lifting-based FBs (L-FBs) for lossy-to-lossless image coding, whose image quality is scalable from lossless to highly compressed lossy data, are not able to use the existing smooth boundary solutions [7–10] because of the rounding error in each lifting step. While our previous work presented a reversible SE (RevSE) for lifting-based LPFBs (L-LPFBs) [11], the nonlinear-phase case has not been treated yet.

This study presents a pseudo RevSE (P-RevSE) for lifting-based nonlinear-phase paraunitary filter banks (L-NLPPUFBs). NLPPUFBs are NLPFBs with paraunitariness and are more practical than NLPFBs without paraunitariness. In addition, NLPPUFBs, whose building blocks are orthonormal matrices, can be easily factorized into lifting structures for lossy-to-lossless image coding because a minimum condition to realize a lifting factorization of a matrix is that the determinant is ± 1 [12]. The P-RevSE is implemented smoothly at the signal boundaries by using a nonexpansive convolution of an SE according to [9] and determinant control for the lifting factorization. Although the determinant control causes a *pseudo* SE, not a *true* SE, the resulting L-NLPPUFB with P-RevSE outperforms not only L-NLPPUFB with PE but also the current LT used in the JPEG XR standard.

Notations: Boldface small and capital letters represent vectors and matrices, respectively. $\mathbf{I}_{[m]}$, $\mathbf{J}_{[m]}$, and $\cdot^T$ mean an $m \times m$ identity matrix, $m \times m$ reversal matrix, and transpose of a matrix, respectively. We omit the matrix sizes when they are obvious.

2. NONLINEAR-PHASE PARAUNITARY FILTER BANKS

Let $M \times MK$ NLPFB ($M, K \in \mathbb{N}$, M is even, $K \geq 2$) be an NLPFB whose channel and filter length are M and MK, respectively. The polyphase matrix $\mathbf{E}(z)$ is expressed as [13]

$$\mathbf{E}(z) = \left(\prod_{i=K-1}^{1} \mathbf{G}_i \mathbf{\Lambda}_i(z) \right) \mathbf{G}_0, \tag{1}$$

where $\mathbf{G}_k$ ($k = 0, 1, \cdots, K-1$) is an $M \times M$ arbitrary nonsingular matrix and $\mathbf{\Lambda}_i(z)$ is a delay matrix with a delay element z as:

$$\mathbf{\Lambda}_i(z) = \begin{bmatrix} \mathbf{I}_{[M-\gamma_i]} & \mathbf{0} \\ \mathbf{0} & z^{-1}\mathbf{I}_{[\gamma_i]} \end{bmatrix}. \tag{2}$$

Although γ_i is an arbitrary integer $1 \leq \gamma_i \leq M-1$, we set $\gamma_i = M/2$ for simplicity. Thus, $\mathbf{\Lambda}_i(z)$ is denoted as $\mathbf{\Lambda}(z)$. Since an NLPFB is not constrained by the linear-phase property, it achieves a better frequency decomposition compared with the linear-phase case. When $\mathbf{G}_k$ is an arbitrary orthonormal matrix, $\mathbf{G}_k^{-1} = \mathbf{G}_k^T$ [5], an NLPFB is called an NLPPUFB.

3. SYMMETRIC EXTENSION FOR NLPPUFBS

Tanaka et al. proposed a nonexpansive convolution for NLPPUFBs [9]. The top images of Fig. 1 shows the upper boundary

This work was supported by JSPS Grant-in-Aid for Young Scientists (B), Grant Number 16K18100.

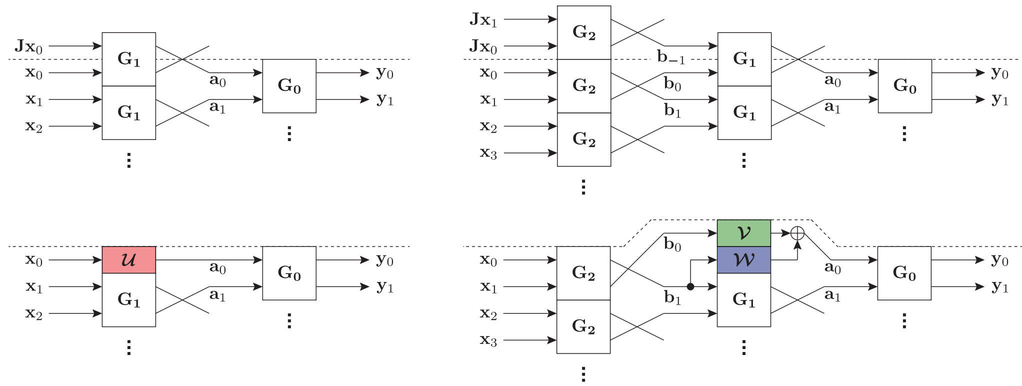

Fig. 1. Upper boundary processing of the analysis banks of NLPPUFBs (dashed lines mean boundaries): (top) SE, (bottom) nonexpansive convolution, (left) $K = 2$, (right) $K = 3$.

processing of the analysis banks of NLPPUFBs when $K = 2$ and 3. They mean that $(K-1)M/2$ extra signals have to be extended at each boundary. To obtain smooth signals and for simplicity, the extra signals are commonly extended by using $\mathbf{J}_{[(K-1)M/2]}$; i.e., the extension is an SE.

Here, we have a nonexpansive problem because the signals transmitted to the synthesis bank should only be $\mathbf{y}_n$ $(n = 0, 1, 2, \cdots)$. This section presents a reconstruction method at the synthesis bank without any extra signal; i.e., $\mathbf{x}_n$ is reconstructed from only $\mathbf{a}_n$, which can be reconstructed from $\mathbf{y}_n$. Let $\mathbf{G}_k$ be

$$\mathbf{G}_k = \begin{bmatrix} \mathbf{A}_k & \mathbf{B}_k \\ \mathbf{C}_k & \mathbf{D}_k \end{bmatrix}, \tag{3}$$

where each submatrix is $M/2 \times M/2$. Hereafter, we consider only the upper boundary processing. The signals at the lower boundary processing can be reconstructed in the same way as in the upper boundary processing.

3.1. Case of $K = 2$

From the top left of Fig. 1, we obtain

$$\mathbf{a}_0 = \begin{bmatrix} \mathbf{A}_1 & \mathbf{B}_1 \end{bmatrix} \begin{bmatrix} \mathbf{Jx}_0 \\ \mathbf{x}_0 \end{bmatrix} = \underbrace{(\mathbf{A}_1\mathbf{J} + \mathbf{B}_1)}_{\triangleq \boldsymbol{\mathcal{U}}} \mathbf{x}_0. \tag{4}$$

The problem is to reconstruct $\mathbf{x}_0$ from $\mathbf{a}_0$, which is transmitted to the synthesis bank. $\mathbf{x}_0$ is represented as

$$\mathbf{x}_0 = \boldsymbol{\mathcal{U}}^{-1}\mathbf{a}_0, \tag{5}$$

where the boundary matrix $\boldsymbol{\mathcal{U}}$ has to be nonsingular, i.e., $\det(\boldsymbol{\mathcal{U}}) \neq 0$. The nonexpansive convolution of the analysis banks in case of $K = 2$ is shown at the bottom left of Fig. 1.

3.2. Case of $K = 3$

From the top right of Fig. 1, similar to the case of $K = 2$, we obtain

$$\mathbf{b}_{-1} = \begin{bmatrix} \mathbf{A}_2 & \mathbf{B}_2 \end{bmatrix} \begin{bmatrix} \mathbf{Jx}_1 \\ \mathbf{Jx}_0 \end{bmatrix} = \begin{bmatrix} \mathbf{B}_2\mathbf{J} & \mathbf{A}_2\mathbf{J} \end{bmatrix} \begin{bmatrix} \mathbf{x}_0 \\ \mathbf{x}_1 \end{bmatrix}. \tag{6}$$

Also, $\mathbf{x}_0$ and $\mathbf{x}_1$ in Eq. (6) can be recalculated from $\mathbf{b}_0$ and $\mathbf{b}_1$ as

$$\begin{bmatrix} \mathbf{x}_0 \\ \mathbf{x}_1 \end{bmatrix} = \underbrace{\begin{bmatrix} \mathbf{A}_2^T & \mathbf{C}_2^T \\ \mathbf{B}_2^T & \mathbf{D}_2^T \end{bmatrix}}_{\mathbf{G}_2^T} \begin{bmatrix} \mathbf{b}_1 \\ \mathbf{b}_0 \end{bmatrix}, \tag{7}$$

where $\mathbf{G}_2$ is an orthonormal matrix. We cannot easily calculate $\mathbf{b}_0$ from the limited signals $\mathbf{a}_n$ unlike $\mathbf{b}_1$. Substituting Eq. (7) into Eq. (6) yields

$$\mathbf{b}_{-1} = \begin{bmatrix} \mathbf{B}_2\mathbf{J} & \mathbf{A}_2\mathbf{J} \end{bmatrix} \begin{bmatrix} \mathbf{A}_2^T & \mathbf{C}_2^T \\ \mathbf{B}_2^T & \mathbf{D}_2^T \end{bmatrix} \begin{bmatrix} \mathbf{b}_1 \\ \mathbf{b}_0 \end{bmatrix}. \tag{8}$$

Also, we obtain

$$\mathbf{a}_0 = \begin{bmatrix} \mathbf{A}_1 & \mathbf{B}_1 \end{bmatrix} \begin{bmatrix} \mathbf{b}_{-1} \\ \mathbf{b}_0 \end{bmatrix}. \tag{9}$$

Consequently, $\mathbf{b}_0$ can be calculated from Eqs. (8) and (9) as

$$\mathbf{b}_0 = \underbrace{\left(\mathbf{A}_1\left(\mathbf{B}_2\mathbf{J}\mathbf{C}_2^T + \mathbf{A}_2\mathbf{J}\mathbf{D}_2^T\right) + \mathbf{B}_1\right)}_{\triangleq \boldsymbol{\mathcal{V}}}^{-1} \cdot \left(\mathbf{a}_0 - \underbrace{\mathbf{A}_1\left(\mathbf{B}_2\mathbf{J}\mathbf{A}_2^T + \mathbf{A}_2\mathbf{J}\mathbf{B}_2^T\right)}_{\triangleq \boldsymbol{\mathcal{W}}}\mathbf{b}_1\right), \tag{10}$$

where the boundary matrix $\boldsymbol{\mathcal{V}}$ has to be nonsingular, i.e., $\det(\boldsymbol{\mathcal{V}}) \neq 0$. The nonexpansive convolution of the analysis banks in case of $K = 3$ is shown at the bottom right of Fig. 1.

For any K, the signals can be reconstructed as the solution of a simultaneous matrix equation with $(K-1)$ unknowns.

4. PSEUDO SYMMETRIC EXTENSION FOR L-NLPPUFBS

This section presents a P-RevSE for L-NLPPUFBs that uses the non-expansive convolution described in Sec. 3 and determinant control for the lifting factorization. From the bottom of Fig. 1, if the structures are expressed as lifting structures, they achieve reversible transforms for lossless image coding. We can consider that the processing with $\boldsymbol{\mathcal{W}}$ is already a lifting structure. Consequently, the residual matrices $\mathbf{G}_k$, $\boldsymbol{\mathcal{U}}$, and $\boldsymbol{\mathcal{V}}$ should be factorized into lifting structures. A minimum condition to realize a lifting factorization of a

Table 1. Coding gain C_{cg}s of the resulting 4×12 L-NLPPUFBs.

Boundary	Not	Upper	Lower
C_{cg}	8.3168	8.2852	8.3173

Table 2. Lossless image coding results (LBR [bpp]).

Test Images	LT [2] RevSE	L-NLPPUFBs PE	P-RevSE
Barbara	4.801	4.798	**4.775**
Boat	5.124	5.103	**5.093**
Elaine	5.166	5.132	**5.106**
Lena	**4.587**	4.615	**4.587**
Pepper	4.954	4.907	**4.897**
Room	**4.344**	4.452	4.427

matrix is that the determinant is ± 1 [12]. Since $\mathbf{G}_k$ is an orthonormal matrix, i.e., $\det(\mathbf{G}_k) = \pm 1$, the matrix can be factorized into lifting structures. On the other hand, note that the determinants of $\mathcal{U}$ and $\mathcal{V}$ might not satisfy this condition, i.e., $\det(\mathcal{U}) \neq \pm 1$ and $\det(\mathcal{V}) \neq \pm 1$. Thus, we control the matrices in

$$\widetilde{\mathcal{U}} = \frac{\mathcal{U}}{\sqrt[M/2]{|\det(\mathcal{U})|}} \quad \text{and} \quad \widetilde{\mathcal{V}} = \frac{\mathcal{V}}{\sqrt[M/2]{|\det(\mathcal{V})|}}, \tag{11}$$

where $\det(\mathcal{U}) \neq 0$ and $\det(\mathcal{V}) \neq 0$, and these conditions are completely equivalent to those as described in Sec. 3. Since these matrices $\widetilde{\mathcal{U}}$ and $\widetilde{\mathcal{V}}$ satisfy the condition for a lifting factorization, $\det(\widetilde{\mathcal{U}}) = \pm 1$ and $\det(\widetilde{\mathcal{V}}) = \pm 1$, $\widetilde{\mathcal{U}}$ and $\widetilde{\mathcal{V}}$ can be factorized into lifting structures. This means that the top half of $\mathbf{G}_1$ at the signal boundaries is scaled by $\sqrt[M/2]{|\det(\mathcal{U})|}$ and $\sqrt[M/2]{|\det(\mathcal{V})|}$,

$$\widetilde{\mathbf{G}_1} = \begin{bmatrix} \frac{1}{s}\mathbf{I} & \mathbf{0} \\ \mathbf{0} & \mathbf{I} \end{bmatrix} \mathbf{G}_1 = \begin{bmatrix} \frac{1}{s}\mathbf{A}_1 & \frac{1}{s}\mathbf{B}_1 \\ \mathbf{C}_1 & \mathbf{D}_1 \end{bmatrix}, \tag{12}$$

where $s = \sqrt[M/2]{|\det(\mathcal{U})|}$ $(K = 2)$ or $\sqrt[M/2]{|\det(\mathcal{V})|}$ $(K = 3)$; i.e., the NLPPUFBs losing the original properties are used at the signal boundaries. Therefore, if $\sqrt[M/2]{|\det(\mathcal{U})|}$ and $\sqrt[M/2]{|\det(\mathcal{V})|}$ are quite different from 1, the boundary processing cannot be implemented smoothly. Accordingly, we have to take this into consideration when designing the NLPPUFB.

5. EXPERIMENTAL RESULTS

5.1. Design of NLPPUFBs

We designed 4×12 ($M = 4$ and $K = 3$) NLPPUFB with the cost function ϕ, which is a weighted linear combination of the coding gain C_{cg} [14], the symmetric property of filters C_{sym} [9], and the determinant control of matrices C_{det}, as follows:

$$\phi = -w_0 C_{cg} + w_1 C_{sym} + w_2 C_{det}, \tag{13}$$

where

$$C_{det} = \left(|\det(\mathcal{V}_u)| - 1\right)^2 + \left(|\det(\mathcal{V}_l)| - 1\right)^2. \tag{14}$$

$\mathcal{V}_u$ and $\mathcal{V}_l$ mean $\mathcal{V}$ at the upper and lower boundary processing of the NLPPUFBs. w_k was experimentally-determined as $\{w_0, w_1, w_2\} = \{1, 0.01, 0.15\}$. Regularity, which is one of the most important image coding properties to prevent the DC leakage, was considered structurally [12]. As described in the previous section, smooth boundary processing cannot be implemented if $\sqrt[M/2]{|\det(\mathcal{V})|}$ is quite different from 1. However, the resulting 4×12 NLPPUFB achieved $\sqrt[M/2]{|\det(\mathcal{V}_u)|} = 0.9339 \approx 1$ and $\sqrt[M/2]{|\det(\mathcal{V}_l)|} = 0.9635 \approx 1$ thanks to the cost functions C_{sym} and C_{det}. Table 1 and Fig. 2 respectively show the coding gain C_{cg}s and the frequency responses of the resulting 4×12 NLPPUFBs at non-signal boundaries, upper signal boundaries, and lower signal boundaries. From the coding gains and frequency responses, we consider that the differences that depend on the signal boundaries are trivial.

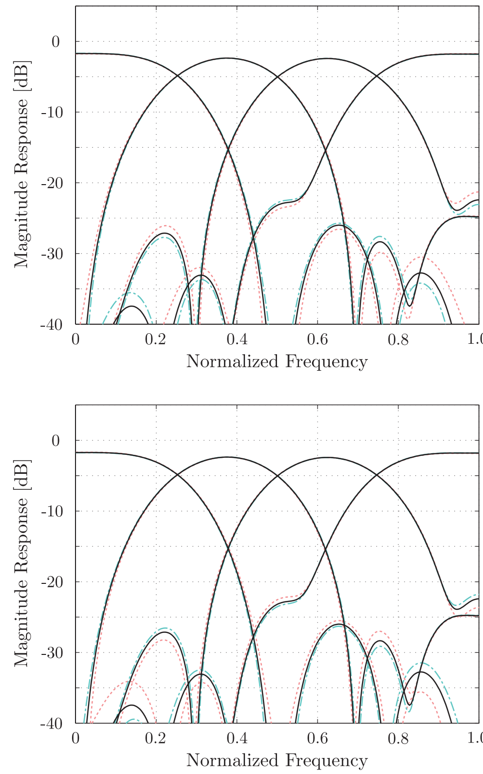

Fig. 2. Frequency responses of the resulting 4×12 NLPPUFBs (black solid, pink dotted, and light blue chained lines mean the NLPPUFBs at non-signal boundaries, upper signal boundaries, and lower signal boundaries, respectively): (top) analysis banks, (bottom) synthesis banks.

5.2. Lossy-to-Lossless Image Coding

We evaluated the 4×8 LT (JPEG XR) with RevSE[1] and the resulting 4×12 L-NLPPUFBs with PE and P-RevSE through lossy-to-lossless image coding. A single-row elementary reversible matrix (SERM) [15] was used for the lifting factorization of $\mathbf{G}_k$ and $\widetilde{\mathcal{V}}$. As described in Sec. 4, the processing with $\mathcal{W}$ is considered to be a lifting structure without any lifting factorization. The resulting 4×12 L-NLPPUFBs were implemented with a rounding operation at each lifting step and compared in terms of the lossless bitrate (LBR) [bpp] in lossless image coding and peak signal-to-noise ratio (PSNR) [dB]

[1]Note that the RevSE in JPEG XR is not equivalent to [11] because it is customized for JPEG XR.

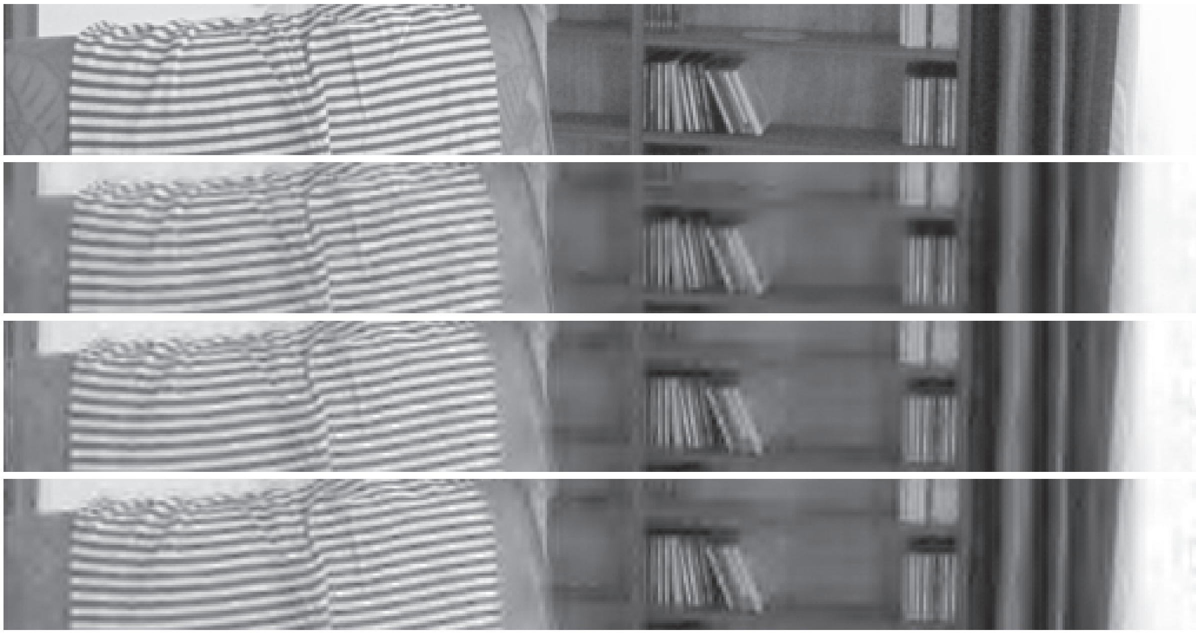

Fig. 3. Particular areas of images of *Room*, which was lossy compressed with 0.25 [bpp] (top and bottom boundaries of each image are non-image boundaries): (top-to-bottom) original image, LT with RevSE, L-NLPPUFB with PE, and L-NLPPUFB with P-RevSE.

Table 3. Lossy image coding results (PSNR [dB]).

Test Images	Bitrate [bpp]	LT [2] RevSE	L-NLPPUFBs PE	L-NLPPUFBs P-RevSE
Barbara	0.25	26.569	27.436	**27.578**
	0.50	30.334	31.097	**31.234**
	1.00	34.952	35.601	**35.728**
Boat	0.25	27.261	28.129	**28.219**
	0.50	30.727	31.296	**31.371**
	1.00	34.213	34.758	**34.805**
Elaine	0.25	30.825	31.178	**31.381**
	0.50	32.502	32.876	**33.016**
	1.00	34.179	34.746	**34.894**
Lena	0.25	31.603	31.965	**32.251**
	0.50	35.024	35.300	**35.524**
	1.00	38.247	38.572	**38.708**
Pepper	0.25	31.026	31.078	**31.586**
	0.50	33.892	34.207	**34.328**
	1.00	35.428	36.200	**36.273**
Room	0.25	27.818	28.684	**29.048**
	0.50	32.715	32.838	**33.116**
	1.00	38.288	37.927	**38.407**

in lossy image coding:

$$\text{LBR [bpp]} = \frac{\text{Total number of bits [bit]}}{\text{Total number of pixels [pixel]}} \tag{15}$$

and

$$\text{PSNR [dB]} = 10 \log_{10} \left(\frac{255^2}{\text{Mean Squared Error}} \right). \tag{16}$$

To evaluate transform performance fairly, we employed two-level decompositions on all transforms. The image set included six 512×512 eight-bit standard grayscale images in [16]. A quadtree-based embedded image coder EZW-IP [17] was used to encode the transformed images.

Table 2, Table 3, and Fig. 3 show the lossless and lossy image coding results. The results show the advantage of the L-NLPPUFB with P-RevSE over the L-NLPPUFB with PE. Especially, in Fig. 3, the L-NLPPUFB with PE produces annoying artifacts, whereas no artifacts are apparent in the image from the L-NLPPUFB with P-RevSE. In addition, the L-NLPPUFB with P-RevSE outperformed the 4×8 LT with RevSE.

6. CONCLUSION

This study presented a P-RevSE for L-NLPPUFBs. The conventional L-NLPPUFBs without any smooth boundary processing have the annoying artifacts at signal boundaries. The L-NLPPUFB with P-RevSE solved this problem by using a nonexpansive convolution of an SE and determinant control for the lifting factorization. Although the determinant control caused a *pseudo* SE, not a *true* SE, the L-NLPPUFB with P-RevSE outperformed not only the L-NLPPUFB with PE but also the current transform used in JPEG XR.

7. REFERENCES

[1] F. Dufaux, G. J. Sullivan, and T. Ebrahimi, "The JPEG XR image coding standard," *IEEE Signal Process. Mag.*, vol. 26, no. 6, pp. 195–199, 204, Nov. 2009.

[2] C. Tu, S. Srinivasan, G. J. Sullivan, S. Regunathan, and H. S. Malvar, "Low-complexity hierarchical lapped transform for

lossy-to-lossless image coding in JPEG XR/HD Photo," in *Proc. of SPIE*, San Diego, CA, Aug. 2008, vol. 7073, pp. 70730C–70730C–12.

[3] T. D. Tran, R. L. de Queiroz, and T. Q. Nguyen, "Linear-phase perfect reconstruction filter bank: Lattice structure, design, and application in image coding," *IEEE Trans. Signal Process.*, vol. 48, no. 1, pp. 133–147, Jan. 2000.

[4] M. J. T. Smith and S. L. Eddins, "Analysis/synthesis techniques for subband image coding," *IEEE Trans. Signal Process.*, vol. 38, no. 8, pp. 1446–1456, Aug. 1990.

[5] X. Gao, T. Q. Nguyen, and G. Strang, "On factorization of M-channel paraunitary filterbanks," *IEEE Trans. Signal Process.*, vol. 49, no. 7, pp. 1433–1446, July 2001.

[6] L. Gan and K. K. Ma, "On simplified order-one factorizations of paraunitary filterbanks," *IEEE Trans. Signal Process.*, vol. 52, no. 3, pp. 674–686, Mar. 2004.

[7] R. L. de Queiroz and K. R. Rao, "On reconstruction methods for processing finite-length signals with paraunitary filter banks," *IEEE Trans. Signal Process.*, vol. 43, no. 10, pp. 2407–2410, Oct. 1995.

[8] R. L. de Queiroz, "Further results on reconstruction methods for processing finite-length signals with perfect reconstruction filter," *IEEE Trans. Signal Process.*, vol. 48, no. 6, pp. 1814–1816, June 2000.

[9] Y. Tanaka, A. Ochi, and M. Ikehara, "A non-expansive convolution for nonlinear-phase paraunitary filter banks and its application to image coding," in *Proc. of ACSSC'05*, Pacific Grove, CA, Oct. 2005.

[10] T. Uto, T. Oka, and M. Ikehara, "M-channel nonlinear phase filter banks in image compression: Structure, design, and signal extension," *IEEE Trans. Signal Process.*, vol. 55, no. 4, pp. 1339–1351, Apr. 2007.

[11] T. Suzuki and M. Ikehara, "Reversible symmetric nonexpansive convolution: An effective image boundary processing for M-channel lifting-based linear-phase filter banks," *IEEE Trans. Image Process.*, vol. 23, no. 6, pp. 2744–2749, June 2014.

[12] T. Suzuki, M. Ikehara, and T. Q. Nguyen, "Generalized block-lifting factorization of M-channel biorthogonal filter banks for lossy-to-lossless image coding," *IEEE Trans. Image Process.*, vol. 21, no. 7, pp. 3220–3228, July 2012.

[13] Y. J. Chen, S. Oraintara, and K. S. Amaratunga, "Theory and factorization for a class of structurally regular biorthogonal filter banks," *IEEE Trans. Signal Process.*, vol. 54, no. 2, pp. 691–700, Feb. 2006.

[14] P. P. Vaidyanathan, *Multirate Systems and Filter Banks*, Englewood Cliffs, NJ: Prentice Hall, 1992.

[15] P. Hao and Q. Shi, "Matrix factorizations for reversible integer mapping," *IEEE Trans. Signal Process.*, vol. 49, no. 10, pp. 2314–2324, Oct. 2001.

[16] "The USC-SIPI Image Database," *Univ. Southern California, Signal and Image Processing Institute [Online]*, Available: http://sipi.usc.edu/database/.

[17] Z. Liu and L. J. Karam, "An efficient embedded zerotree wavelet image codec based on intraband partitioning," in *Proc. of ICIP'00*, Vancouver, British Columbia, Canada, Sep. 2000.